Nucleic Acids Research, 1999, Vol. 27, No. 16 **3283–3290**

Facile characterization of translation initiation via nonsense codon suppression

Andrei V. Karginov, Michiel Lodder and Sidney M. Hecht*

Department of Chemistry and Department of Biology, University of Virginia, Charlottesville, VA 22901, USA

Received May 10, 1999; Revised and Accepted June 23, 1999

ABSTRACT

A new strategy for studying the mechanism of translation initiation in eukaryotes has been developed. The strategy involves the use of an *in vitro* translation system to incorporate a non-natural fluorescent amino acid into a protein from a suppressor $tRNA^{Phe}_{CUA}$ misacylated with that amino acid. It is thereby possible to monitor translation initiation efficiency at an AUG codon in different contexts; this is illustrated for three constructs encoding *Escherichia coli* dihydrofolate reductase mRNA with different translation initiation regions. Fluorescence measurements after *in vitro* translation of the mRNAs in rabbit reticulocyte lysate reflected differences in the position and efficiency of translation initiation and, therefore, can be used for characterization of the translation initiation process.

INTRODUCTION

Translation initiation is a key regulatory step in the synthesis of numerous proteins in eukaryotic cells. Different forms of the same protein, sometimes having distinct functions, can be produced as a result of alternative initiation of translation (1–4). It has also been found that translation reinitiation is involved in regulation of the viral life cycle for human immunodeficiency virus type 1 (5–7).

The current model of translation initiation in eukaryotes posits the start of protein synthesis at the AUG codon nearest to the 5'-end of the mRNA (8–13). In some cases, reinitiation of translation can occur at the next AUG codon following translation termination (14–16). Another process, called 'leaky scanning', takes place when the 40S ribosomal subunits bypass the first AUG codon because it is present in a non-optimal codon context. In this case the ribosomes initiate synthesis at a downstream AUG codon (10–13,16).

In spite of the fact that the described translation initiation mechanism was shown to predominate for normal eukaryotic mRNAs, some viruses, such as hepatitis C virus (HCV), Moloney murine leukemia virus (MoMuLV), encephalomyocarditis virus (EMCV), foot-and-mouth disease virus (FMDV) and poliovirus, use an unusual internal translation initiation process (17–22). The same mechanism was described recently for translation of the human proto-oncogene c-myc (23). In this case, protein synthesis starts far (>400 nt) from the 5'-end, which can hardly be explained by 'leaky scanning' or 'stop and reinitiation' mechanisms.

A powerful technique for incorporation of synthetic amino acids into a protein at a predetermined position has been developed within the last two decades. The method involves incorporation of a stop codon at the position of interest in the protein gene and *in vitro* expression of the gene in the presence of misacylated suppressor tRNA, the latter of which participates in read-through of the stop codon (24–36). Numerous modified proteins and peptides have been synthesized successfully and studied using this strategy (34–41). Another recent achievement utilizing misacylated suppressor tRNAs involved exploration of the translation initiation mechanism via *in vitro* suppression (42). It was shown that different types of translation initiation (e.g. reinitiation, 'leaky scanning') can be regulated and distinguished by varying the concentration of the misacylated tRNA.

Here we describe a system that has the potential to facilitate the study of the position and efficiency of translation initiation in eukaryotic cells and the identification of inhibitors of specific translation initiation mechanisms for some viruses. The strategy is based on *in vitro* suppression and employs a suppressor tRNA misacylated with 3-*N*-(7-nitrobenz-2-oxa-1,3-diazol-4-yl)-2,3-diaminopropionic acid (NBD-Dap) (Scheme 1) in a protein synthesis reaction as a marker and potential regulator (42) of translation.

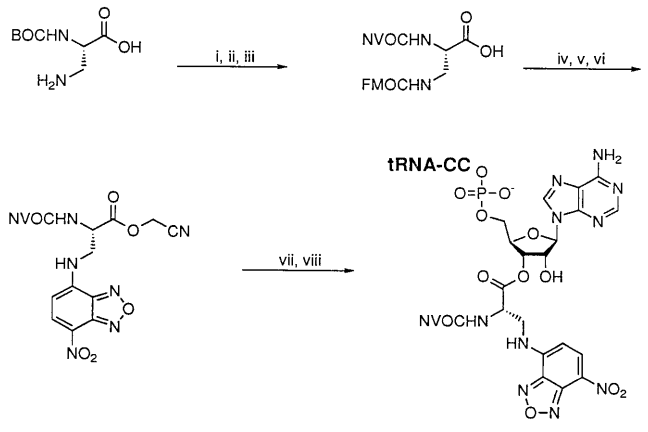

Scheme 1. (i) FMOC succinimide; (ii) 4 N HCl in dioxane; (iii) 6-nitroveratryl chloroformate; (iv) piperidine; (v) NBD chloride; (vi) chloroacetonitrile; (vii) pdCpA; (viii) tRNA-C_{OH}, T4 RNA ligase.

*To whom correspondence should be addressed. Tel: +1 804 924 3906; Fax: +1 804 924 7856; Email: sidhecht@virginia.edu

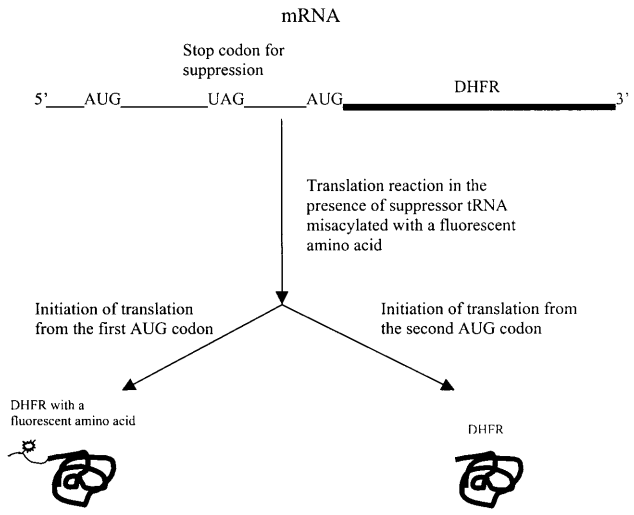

Figure 1. Alternative initiation of translation of DHFR. Only full-length translation product gives a fluorescence signal.

An outline of the strategy is presented in Figure 1. Initiation of translation at the first AUG codon results in production of full-length dihydrofolate reductase (DHFR) including the fluorescent amino acid. Initiation of translation from the second AUG codon produces a truncated protein, which does not include the fluorescent amino acid. Therefore, by comparing the intensity of the fluorescence signal with the amount of DHFR protein produced it is possible to monitor the extent to which translation is initiated at the first AUG codon, as well as the overall efficiency of the process.

MATERIALS AND METHODS

[^{35}S]methionine (1000 Ci/mmol) was purchased from Amersham Corp. Nuclease-treated rabbit reticulocyte lysate system, T7 transcription kit and restriction endonucleases were obtained from Promega Inc. T4 DNA ligase and T4 RNA ligase were obtained from New England Biolabs. Synthetic oligonucleotides were obtained from Gibco BRL and Cruachem, Inc. The Sequenase v.2.0 DNA sequencing kit was purchased from US Biochemical. NBD chloride was purchased from Aldrich; DEAE Sepharose CL-6B was from Sigma.

UV spectral measurements were made using a Perkin-Elmer Lambda Array 3840 spectrophotometer. Radioactivity measurements were performed with a Beckman LS-100C liquid scintillation counter. Phosphorimager analysis was performed using a Molecular Dynamics 300E phosphorimager equipped with ImageQuant software. Fluorescence measurements were made using a Fluorolog 2 fluorescence spectrophotometer (Jobin Yvon SPEX Inc.) and a Molecular Dynamics fluorimager equipped with ImageQuant software.

Run-off transcription of truncated yeast $tRNA^{Phe}_{CUA}$ (–CA) and mRNAs was carried out as described (41).

Construction of plasmids for DHFR gene *in vitro* expression

Plasmid pTHD8, a derivative of plasmid pTZRKE (41), encoding a hexahistidine–DHFR fusion protein under the control of the T7 and *lac* promoters (Fig. 2A), was modified for this study. The *Hin*dIII–*Pfl*MI fragment from pTHD8 coding for the *lac* promoter, a hexahistidine-containing peptide and the first 19 amino acids of DHFR was replaced by a synthetic oligonucleotide duplex coding for a hexahistidine-containing peptide, a UAG site for suppression (for three suppression constructs) or GCG sequence (for wild-type constructs), a TEV protease cleavage site, the first 19 amino acids of DHFR and different 5'-untranslated regions, as described in Results. In total, six constructs were prepared. The plasmids were denoted pOpt, pOptC, pNopt, pNoptC, pAlt and pAltC (Fig. 2B). The nucleotide sequences of all of the plasmids were verified by restriction analysis and Sanger DNA sequencing (43).

In vitro synthesis of DHFR

In a typical experiment, DHFR was synthesized in a reaction mixture (10–100 µl total volume) that contained, per 100 µl: 70 µl of nuclease-treated rabbit reticulocyte lysate, 80 µCi of [^{35}S]*S*-methionine (1000 Ci/mmol), 5 µl of a 1 mM solution of all 20 amino acids, 20 µg of the appropriate mRNA and 20 µg of deprotected aminoacyl-$tRNA^{Phe}_{CUA}$. The reaction mixture was incubated at 30°C for 1.5 h. *In vitro* translation of control mRNAs was carried out without added misacylated tRNA. Aliquots (1 µl) were analyzed by 13% SDS–PAGE (44). Analysis and quantification of bands was carried out using a phosphorimager.

Purification of the recombinant DHFR

In vitro translation mixture (200 µl) containing (putatively fluorescent) ^{35}S-labeled protein or 0.05 A_{260} U of NBD-Dap–pdCpA as a control for fluorescence background was incubated with 1 µg of RNase A for 30 min at room temperature and then applied to a 200 µl DEAE Sepharose CL-6B column that had been equilibrated with 5 mM K phosphate buffer, pH 7.0. The column was washed with four 400 µl portions of 5 mM K phosphate buffer, pH 7.0, then with three 400 µl portions of 5 mM K phosphate buffer, pH 7.0, containing 100 mM KCl, and finally with three 400 µl portions of 5 mM K phosphate buffer, pH 7.0, containing 150 mM KCl. The remaining proteins were washed from the column with 800 µl of 5 mM K phosphate buffer, pH 7.0, containing 0.4 M KCl. The fluorescence emission signal was measured at 545 nm (excitation wavelength 480 nm). The purified material was analyzed by 13% SDS–PAGE (44) and scanned on a fluorimager (excitation at 488 nm, emission at 570 nm).

Synthesis of protected NBD-Dap–pdCpA and misacylated tRNAs

N^{β}-9-Fluorenylmethoxycarbonyl-(S)-diaminopropionic acid. To a solution containing 750 mg (3.67 mmol) of N^{α}-butyloxycarbonyl-(*S*)-diaminopropionic acid and 606 mg (3.67 mmol) of K_2CO_3 in 10 ml of H_2O and 5 ml of dioxane was added a solution of 1.36 g (4.04 mmol) of FMOC succinimide in 5 ml of dioxane. The mixture was stirred at room temperature for 24 h, diluted with 25 ml of H_2O and washed with two 25-ml portions of ether. The aqueous phase was acidified to pH 2 with 1 N $NaHSO_4$ and extracted with three 25-ml portions of CH_2Cl_2. The combined extract was dried ($MgSO_4$) and concentrated under diminished pressure. The crude compound was dissolved in 9 ml of 4 N HCl in dioxane. After stirring at room temperature for 2 h, the reaction mixture was concentrated under diminished pressure. Crystallization from MeOH/ether

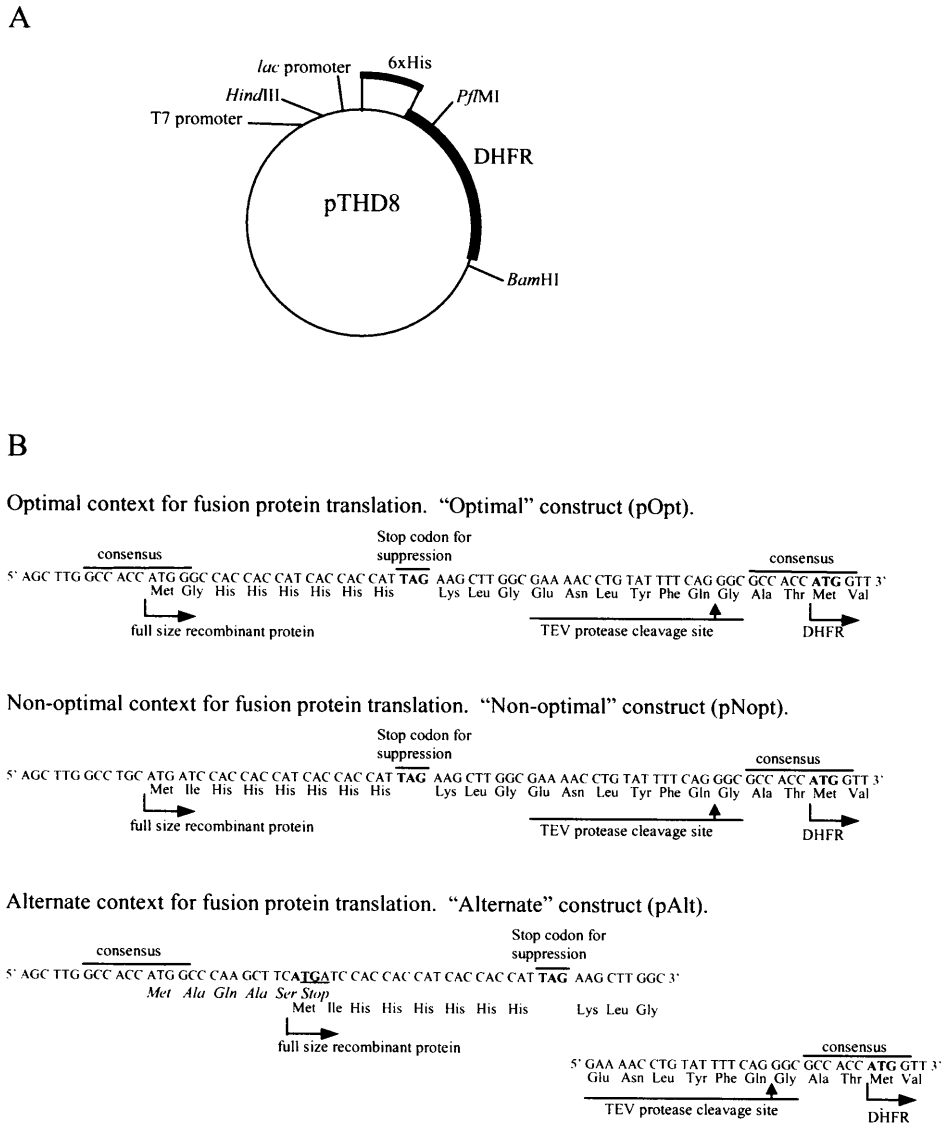

Figure 2. (**A**) Plasmid pTHD8 used for preparation of the six constructs employed in this study. (**B**) The 'optimal' construct contains the first ATG codon in a favorable context (consensus sequence). The 'non-optimal' construct contains the first ATG codon in a suboptimal context (G in position +4 substituted to A, C in position –2 substituted to G, A in position –3 substituted to T). G in position +5 was changed to T to conserve the physicochemical character of the derived fusion protein. The 'alternate' construct contains the first in-frame DHFR start codon overlapping with the stop codon of an upstream mini-cistron. The control constructs were the same in each case except that the TAG codon was replaced by GCG.

gave N^{β}-9-fluorenylmethoxycarbonyl-(*S*)-diaminopropionic acid as a fine colorless powder: yield 1.09 g (82%); mp 234–235°C; ^{1}H NMR (MeOD) δ 3.54 (dd, 1H, *J* = 16 Hz, 6 Hz), 3.68 (dd, 1H, *J* = 14 Hz, 4 Hz), 4.02–4.04 (m, 1H), 4.17–4.19 (m, 1H), 4.32–4.36 (m, 2H), 7.25 (t, 2H, *J* = 7 Hz), 7.34 (t, 2H, *J* = 7 Hz), 7.60 (d, 2H, *J* = 7 Hz) and 7.74 (d, 2H, *J* = 7 Hz). Analysis calculated for $C_{18}H_{19}N_2O_4Cl$: C, 59.59; H, 5.28. Found: C, 59.57; H, 5.27.

N^{α}-6-Nitroveratryloxycarbonyl-N^{β}-9-fluorenylmethoxycarbonyl-(S)-diaminopropionic acid. To a solution containing 550 mg (1.52 mmol) of N^{β}-9-fluorenylmethoxycarbonyl-(*S*)-diaminopropionic acid and 502 mg (3.04 mmol) of K_2CO_3 in 5 ml of H_2O and 5 ml of dioxane was added 480 mg (1.74 mmol) of 6-nitroveratryl chloroformate. The reaction mixture was stirred at room temperature for 17 h, diluted with 25 ml of 1 N $NaHSO_4$ and extracted with three 25-ml portions of CH_2Cl_2. The combined organic extract was dried ($MgSO_4$) and concentrated under diminished pressure. Crystallization from acetone/hexanes gave N^{α}-6-nitroveratryloxycarbonyl-N^{β}-9-fluorenylmethoxycarbonyl-(*S*)-diaminopropionic acid as a colorless solid: yield 673 mg (78%); mp 208–209°C; ^{1}H NMR ($CDCl_3$/MeOD) δ 3.25–3.45 (m, 2H), 3.67 (s, 3H), 3.69 (s, 3H) 3.92–4.18 (m, 4H), 5.23 (dd, 2H, *J* = 10 Hz, 6 Hz), 6.84 (s, 1H), 7.07 (t, 2H, *J* = 7 Hz), 7.14 (t, 2H, *J* = 7 Hz), 7.34 (d, 2H, *J* = 7 Hz), 7.43 (s, 1H) and 7.50 (d, 2H, *J* = 7 Hz).

N^{α}-6-Nitroveratryloxycarbonyl-N^{β}-NBD-(S)-diaminopropionic acid. To a solution containing 250 mg (0.44 mmol) of N^{α}-6-nitroveratryloxycarbonyl-N^{β}-9-fluorenylmethoxycarbonyl-(*S*)-diaminopropionic acid in 3 ml of CH_2Cl_2 was added 0.5 ml of piperidine. After stirring at room temperature for 45 min the reaction mixture was concentrated under diminished pressure. The residue was precipitated from MeOH/ether and dried under diminished pressure to ensure complete removal of piperidine. The residue was suspended in 2 ml of H_2O and 4 ml of methanol and 74 mg (0.88 mmol) of $NaHCO_3$ were added, followed by 110 mg (0.55 mmol) of NBD chloride. After stirring at room temperature for 3 h, another 100-mg portion of NBD chloride was added. After 16 h the reaction mixture was diluted with 25 ml of 1 N $NaHSO_4$ and extracted with three 25-ml portions of CH_2Cl_2. The combined extract was dried ($MgSO_4$) and concentrated under diminished pressure. The crude product was applied to a silica gel column (20 × 2 cm); elution with 3% acetic acid in ethyl acetate gave N^{α}-6-nitroveratryloxycarbonyl-N^{β}-NBD-(*S*)-diaminopropionic acid as an orange solid: yield 60 mg (27%); ^{1}H NMR ($CDCl_3$/MeOD) δ 3.09–3.11 (m, 2H), 3.70 (s, 3H), 3.71 (s, 3H), 4.29–4.31 (m, 1H), 5.25 (s, 2H), 6.17 (d, 1H, *J* = 8 Hz), 6.83 (s, 1H), 7.46 (s, 1H) and 8.23 (d, 1H, *J* = 8 Hz); mass spectrum (FAB) *m/z* 507.1092 $(M+H)^+$ ($C_{19}H_{19}N_6O_{11}$ requires 507.1112).

N^{α}-6-Nitroveratryloxycarbonyl-N^{β}-NBD-(S)-diaminopropionic acid cyanomethyl ester. To a solution containing 45 mg (0.089 mmol) of N^{α}-6-nitroveratryloxycarbonyl-N^{β}-NBD-(*S*)-diaminopropionic acid in 2 ml of acetonitrile was added 62 µl (45 mg, 0.45 mmol) of triethylamine, followed by 56 µl (67 mg, 0.89 mmol) of chloroacetonitrile. After stirring at room temperature for 4 days the mixture was diluted with 25 ml of CH_2Cl_2 and washed with two 25-ml portions of 1 N $NaHSO_4$. The organic layer was dried ($MgSO_4$) and concentrated under diminished pressure. The crude product was applied to a silica gel column (10 × 1 cm); elution with ethyl acetate gave N^{α}-6-nitroveratryloxycarbonyl-N^{β}-NBD-(*S*)-diaminopropionic acid cyanomethyl ester as a yellow solid: yield 30 mg (62%); ^{1}H NMR (acetone-d_6) δ 3.83 (s, 3H), 3.84 (s, 3H), 3.95–4.00 (m, 2H), 4.72–4.77 (m, 3H), 5.38 (s, 2H), 6.30 (d, 1H, *J* = 9 Hz), 6.78 (d, 1H, *J* = 7 Hz), 6.88 (s, 1H), 7.48 (br, 1H), 7.56 (s, 1H) and 8.35 (d, 1H, *J* = 8 Hz); mass spectrum (FAB) *m/z* 546.1197 $(M+H)^+$ ($C_{21}H_{20}N_7O_{11}$ requires 546.1221).

N^{α}-6-Nitroveratryloxycarbonyl-N^{β}-NBD-(S)-diaminopropionic acid pdCpA ester. To a conical vial containing 4.0 mg (2.94 µmol) of the tris(tetrabutylammonium) salt of pdCpA was added 8.0 mg (14.7 µmol) of N^{α}-6-nitroveratryloxycarbonyl-N^{β}-NBD-(*S*)-diaminopropionic acid cyanomethyl ester in 50 µl of DMF. The reaction mixture was stirred at room temperature for 16 h. A 5-µl aliquot of the mixture was diluted with 45 µl of 1:1 CH_3CN/50 mM NH_4OAc, pH 4.5. A sample of 10 µl of the diluted aliquot was analyzed by HPLC on a C_{18} reversed phase column (250 × 10 mm). The column was washed with 1–63% CH_3CN in 50 mM NH_4OAc, pH 4.5, over a period of 45 min at a flow rate of 3.5 ml/min (monitoring at 260 nm). The reaction mixture was diluted to a total volume of 500 µl of 1:1 CH_3CN/50 mM NH_4OAc, pH 4.5, and purified using the same semi-preparative C_{18} reversed phase column [retention times 23.1 and 23.4 min for the two positional (2' and 3') isomers]. After lyophilization, N^{α}-6-nitroveratryloxycarbonyl-N^{β}-NBD-(*S*)-diaminopropionic acid pdCpA ester was obtained as a yellow solid: yield 1.3 mg (39%); mass spectrum (FAB) *m/z* 1125.2114 $(M+H)^+$ ($C_{38}H_{43}N_{14}O_{23}P_2$ requires 1125.2101).

N^{α}-(4-Pentenoyl)-N^{β}-NBD-(S)-diaminopropionic acid pdCpA ester. The 4-pentenoyl-protected pdCpA compound was prepared according to the same scheme as the 6-nitroveratryl-oxycarbonyl-protected compound. The 4-pentenoyl group was introduced as described previously (45).

Preparation of misacylated tRNAs. Ligation reactions were carried out in 50 µl (total volume) of 50 mM Na HEPES buffer, pH 7.5, containing 25 µg of $tRNA^{Phe}_{CUA}$ (–CA) (41), 0.5 A_{260} U (~20 nmol) of an N^{α}-protected aminoacyl-pdCpA, 0.5 mM ATP, 15 mM $MgCl_2$, 20% dimethylsulfoxide (DMSO) and 100 U of T4 RNA ligase. Reaction mixtures were incubated at 37°C for 25 min and then quenched by the addition of 5 µl of 3 M Na acetate, pH 4.5. The (aminoacylated) tRNA was precipitated with 2.5 vol of ethanol, collected by centrifugation, washed with 70% ethanol and dried. The product was redissolved in 1 mM K acetate, pH 4.5, at a final concentration of 0.5 µg/µl and then irradiated with a 500 W mercury/xenon lamp using Pyrex and water filters for 2 min to remove the nitroveratryloxycarbonyl (NVOC) protecting group. Deprotection of the pentenoyl-protected aminoacyl-tRNA was performed by addition of 0.25 vol of 25 mM I_2 in THF/H_2O solution (1:1) and incubation at room temperature for 10 min. The deprotected aminoacyl-tRNA was precipitated with ethanol, washed with 70% ethanol, dried and then redissolved in 1 mM K acetate, pH 4.5, or in 25% DMSO to a final concentration of 2 µg/µl and used in *in vitro* suppression experiments immediately following deprotection.

The extent of ligation to afford misacylated tRNAs was determined by electrophoresis on an 8% polyacrylamide gel (100 × 80 × 0.8 mm) containing 7 M urea in 100 mM Na acetate buffer, pH 4.5, at 200 V for 2 h (46).

RESULTS

Three DNA constructs (‘optimal’, ‘non-optimal’ and ‘alternate’) were created for the *in vitro* suppression experiments (Fig. 2B). Each construct contained the DHFR gene under the control of a T7 promoter. Two start codons for DHFR synthesis were present in each mRNA synthesized from the plasmids. The first ATG codon for the optimal construct is in a favorable context, so translation should start very efficiently at that position. In the non-optimal construct, the first start codon is in a suboptimal context, so some 40S ribosomal subunits may initiate protein synthesis at the second ATG codon. The alternate construct contains an upstream ATG codon in a favorable context and in a reading frame different than that for DHFR; the second upstream ATG codon in the same reading frame as DHFR also overlaps with the TGA termination codon for the preceding mini-cistron. It has been shown by Kozak that translation at an ATG codon positioned in the same fashion as the second ATG codon in this construct occurs very inefficiently (14).

For each of the constructs described a control construct was created as well (‘optimal/control’, ‘non-optimal/control’ and ‘alternate/control’). The control constructs had the same structure as the suppression constructs, except that the TAG codon

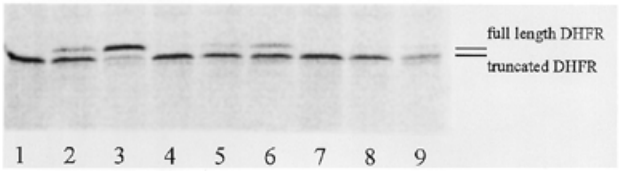

Figure 3. *In vitro* synthesis of DHFR in the presence of valyl-tRNA$^{Phe}_{CUA}$. Protein synthesis was carried out in the presence of [^{35}S]methionine using a rabbit reticulocyte lysate. Lane 1, translation of optimal mRNA without valyl-tRNA$^{Phe}_{CUA}$; lane 2, translation of optimal mRNA in the presence of deprotected valyl-tRNA$^{Phe}_{CUA}$; lane 3, translation of optimal/control mRNA; lane 4, translation of non-optimal mRNA without valyl-tRNA$^{Phe}_{CUA}$; lane 5, translation of non-optimal mRNA in the presence of deprotected valyl-tRNA$^{Phe}_{CUA}$; lane 6, translation of non-optimal/control mRNA; lane 7, translation of alternate mRNA without valyl-tRNA$^{Phe}_{CUA}$; lane 8, translation of alternate mRNA in the presence of deprotected valyl-tRNA$^{Phe}_{CUA}$; lane 9, translation of alternate/control mRNA.

used for suppression was changed to GCG, which codes for alanine.

The DNA constructs were obtained by modification of plasmid pTHD8 (Fig. 2A), which contains the gene for *Escherichia coli* DHFR under control of a T7 promoter. Six different sequences, coding for the first start codon of the DHFR gene in a desired context, followed by the hexahistidine sequence, a suppression stop codon (for suppression constructs), a TEV protease cleavage site and the first 19 amino acids of DHFR, were inserted into the plasmid between *Hin*dIII and *Pfl*MI restriction sites, replacing the original nucleotides. Each of the mRNAs was obtained by run-off *in vitro* transcription of *Bam*HI-linearized plasmid DNA.

A modified yeast tRNA^{Phe} transcript (30,47), containing a CUA anticodon, was chosen as the suppressor tRNA for the *in vitro* experiments. A truncated form of the tRNA lacking the 3'-terminal pCpA was prepared by *in vitro* T7 transcription of linearized pY8 plasmid DNA (41), bearing a gene for the yeast tRNA$^{Phe}_{CUA}$. Aminoacylation of the truncated suppressor tRNA was performed by a modification of published methods (25,34) using T4 RNA ligase-mediated coupling of *N*-protected 2'(3')-*O*-aminoacyl-pdCpA (Scheme 1).

In order to check the translation and suppression efficiencies for the constructs created, valyl-tRNA$^{Phe}_{CUA}$ was employed in the first set of *in vitro* translation experiments (Fig. 3). The suppression efficiencies and the ratios of full-length to total DHFR protein produced (full-length and truncated) for both control ('wild-type') and suppression constructs are presented in Table 1. The ratio of full-length to total DHFR protein produced was chosen as a characteristic value for measuring efficiency of translation initiation at the first AUG codon of the recombinant DHFR gene. The calculations were performed by phosphorimager quantification of radioactivity for the appropriate protein band in the polyacrylamide gel image. As expected, for the optimal and optimal/control constructs, the translation initiation efficiency at the first start codon was much higher than in the case of the non-optimal and non-optimal/control constructs. Alternate and alternate/control constructs produced very small amounts of full-length protein. The amount of full-length fusion protein produced was limited, of course, by the efficiency of suppression of the UAG codon in each construct. Suppression efficiency was 34% for the optimal construct and 40% for the non-optimal construct. Thus, the model system for monitoring alternate translation initiation functioned as designed.

Table 1. *In vitro* translation initiation efficiency data for experiments using valyl-tRNA$^{Phe}_{CUA}$

Construct	Ratio of full-length to total translation product (translation initiation efficiency) (%)
Optimal	24
Non-optimal	11
Alternate	–[a]
Optimal/control	78
Non-optimal/control	21
Alternate/control	11

[a]Not detected (<3%).

In vitro suppression reactions with NBD-Dap–tRNA$^{Phe}_{CUA}$ were subjected to detailed optimization. The optimal mRNA and misacylated suppressor tRNA$^{Phe}_{CUA}$ concentrations were both found to be 0.2 mg/ml. In order to improve suppression efficiency, the translation reactions were carried out at different concentrations of DMSO (1–3%). The suppression efficiency increased with increasing DMSO concentration up to 2.5%, but overall translation efficiency decreased continuously. The optimal DMSO concentration was found to be 2–2.5%. The suppression efficiency in this case increased from 10 (no DMSO) to 27% (2.5% DMSO) for the optimal construct, while translation efficiency decreased from 100 to 66% (Table 2).

Table 2. *In vitro* translation of optimal and optimal/control mRNAs in the presence of DMSO[a]

	Without DMSO	2% DMSO	2.5% DMSO
Suppression efficiency (%)	10	21	27
Translation efficiency (%)[b]	100	78	66

[a]Translation and suppression efficiencies were determined in the presence of NBD-Dap–tRNA$^{Phe}_{CUA}$.

[b]Translation efficiencies are expressed relative to the value obtained in the absence of DMSO.

As described by Turcatti *et al.* (48), NBD-Dap–tRNA$^{Phe}_{CUA}$ protected at the N^{α}-position of the amino acid was more stable to hydrolysis than the deprotected analog. Two different protecting groups were employed, namely the NVOC (31) and pentenoyl groups (45), which can be removed from the derived misacylated tRNA via light or chemical (iodine) treatment, respectively. Experiments with the optimal construct showed that misacylated tRNAs prepared with either of the two protecting groups gave essentially the same level of suppression efficiency.

To obtain enough material for fluorescence measurements, translation of optimal and non-optimal mRNAs in the presence of suppressor NBD-Dap–tRNA$^{Phe}_{CUA}$ was performed on a

200 µl scale in 2.5% DMSO. Translation of the other constructs was carried out on a 20 µl scale. The translation initiation efficiency data are presented in Table 3; suppression efficiencies for the optimal and non-optimal constructs were 24 and 27%, respectively. The translation products from the optimal and non-optimal mRNAs were purified by chromatography on DEAE Sepharose CL-6B to remove fluorescent by-products and hemoglobin; the yield of purified material recovered from the column was 90%. A control sample of 200 µl of rabbit reticulocyte lysate translation mixture, containing NVOC-protected NBD-Dap–pdCpA instead of NBD-Dap–$tRNA^{Phe}_{CUA}$, was subjected to the same purification procedure. The fluorescence signal from the full-length recombinant DHFR was detected using a fluorimager (Fig. 4A).

Table 3. *In vitro* translation initiation efficiency data for experiments using NBD-Dap–$tRNA^{Phe}_{CUA}$[a]

Construct	Ratio of full-length to total translation product (translation initiation efficiency) (%)
Optimal	21
Non-optimal	5
Alternate	–[b]
Optimal/control	86
Non-optimal/control	31
Alternate/control	–[b]

[a]Translation was performed in the presence of 2.5% DMSO.
[b]Not detected (<3%).

The fluorescence signals for the purified translation products were measured at 545 nm (excitation at 480 nm). After subtraction of background, the fluorescence signal for the optimal sample was 3.3 times greater than that for the non-optimal sample (in good agreement with the 3.2 times difference obtained by measurement of radioactivity from the gel) (Table 4). The ratio of fluorescence signal to total DHFR protein was 4.6 times greater for the optimal than for the non-optimal mRNA, again in good agreement with the value of 4.5 determined from the detection of radioactivity in individual bands on a polyacrylamide gel (Fig. 4B).

Table 4. Quantification results for the purified translation products

	Radioactivity[a] (pixels)	Fluorescence[b] (arbitrary units)
Optimal	4638	934
Non-optimal	1457	287

[a]Radioactivity signal was obtained by phosphorimager quantification of the appropriate band in the polyacrylamide gel.
[b]The fluorescence data are given after subtraction of the background signal.

DISCUSSION

As shown previously (42), it is possible to use *in vitro* suppression techniques to study translation initiation. All three basic mechanisms of translation initiation (initiation at the first AUG codon, 'leaky scanning' and 'stop and reinitiation') were observed in the same reaction mixture and regulation of the position of translation initiation was accomplished by changing the concentration of aminoacylated suppressor tRNA (42). Of particular interest was the development of a method that would make detection and analysis of the position and efficiency of translation initiation easier and faster using an *in vitro* suppression strategy. One of the most sensitive and efficient methods of detection utilizes fluorescence. A number of fluorescent unnatural amino acids have been employed for incorporation into a protein during *in vitro* translation (48–50). The use of NBD-Dap resulted in better suppression efficiency than the other amino acids described (48). This compound also has suitable fluorescence parameters, as regards excitation and emission wavelengths; critically these are not obscured by the intrinsic protein fluorescence.

The goal of this study was to model three different examples of alternative translation initiation and check the possibility of detecting and distinguishing translation efficiency from different start codons by fluorescence measurement, using *in vitro* suppression with a tRNA aminoacylated with NBD-Dap. The plasmid DNA constructs (Fig. 2) described above were designed for that purpose. As shown by Kozak (14), initiation of translation occurs most efficiently if the AUG codon is in a favorable context (consensus sequence). Mutations in the consensus sequence can cause a 2- to 3-fold decrease in translation initiation efficiency at that position. The most inefficient translation initiation of full-length DHFR fusion protein occurred when the AUG initiation codon for this protein overlapped with the TGA termination codon of an upstream minicistron whose ATG codon was placed in a favorable context. The results obtained in *in vitro* translation experiments with our designed constructs (Fig. 3 and Table 1) are in good agreement with the current model of initiation of translation in eukaryotes (10).

The major problem with fluorescence measurements is usually the background signal, caused by light scattering and intrinsic fluorescence of some proteins and macromolecules present in the translation mixture. Therefore, in order to maximize the signal-to-noise ratio the optimization of the reaction conditions to obtain the highest possible yield of the derivatized protein was an important step. It is interesting that the addition of DMSO improved the suppression efficiency to almost the same extent as could be achieved by increasing suppressor NBD-Dap–$tRNA^{Phe}_{CUA}$ concentration (data not shown). It is possible that the presence of DMSO increased the solubility of the aminoacyl-tRNA in the translation mixture. The addition of DMSO also improved translation initiation at the first AUG codon, which is reflected in the experiments with the non-optimal/control mRNA (Tables 1 and 3). Translation initiation at the first start codon was 1.5 times more efficient in 2.5% DMSO than in the absence of DMSO for this construct. This observed effect could be due to any number of structural changes in the components of the protein biosynthesizing system.

As described in Results, the fluorescence signal for the optimal translation product was 3.3 times greater than that for the non-optimal product, whereas the difference calculated by radioactivity quantification from the gel was 3.2-fold (Table 4). It may be noted that these numbers could be obtained reliably in

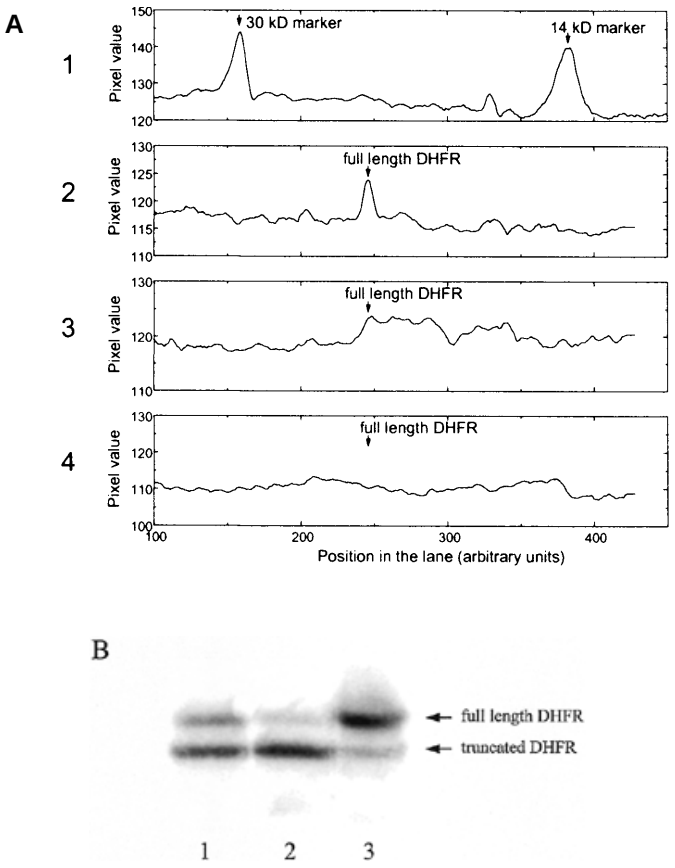

Figure 4. Detection of the fluorescent DHFR fusion protein. (**A**) Image obtained by scanning the gel on a fluorimager. Panel 1, molecular weight markers; panel 2, optimal translation; panel 3, non-optimal translation; panel 4, optimal/control translation. (**B**) Image of the same gel obtained using a phosphorimager. Lane 1, optimal translation; lane 2, non-optimal translation; lane 3, optimal/control translation. All translation mixtures were purified on DEAE Sepharose CL-6B.

spite of the high fluorescence background in the gel (~3500 arbitrary units; Fig. 4A). The similarity of these two values indicates that one may use the ratio of fluorescence signal to total DHFR protein produced as a characteristic value that reflects changes in translation initiation efficiency at the first AUG codon. Indeed, the ratio of fluorescence signal to the total amount of the DHFR protein produced was 4.6 times greater for optimal translation product than for non-optimal, which is again very close to the value of 4.5 calculated by quantification of the protein bands in the polyacryamide gel (Fig. 4).

While the protein was purified in the present case to ensure accuracy of measurements and obviate the possibility of interference from components of the protein biosynthesizing system, it is anticipated that fluorescence measurements could be recorded directly using proteins derived from an appropriately constituted system.

Therefore, this method is reliable enough to monitor translation initiation at different positions of an mRNA and to determine the efficiency of initiation. The use of a fluorescent amino acid in the *in vitro* suppression experiments makes the analysis of the results easier and faster. The system described can also potentially be employed to study alternative translation initiation mechanisms and factors affecting the position and efficiency of translation initiation for numerous mammalian genes as well as for human immunodeficiency virus type 1 tat mRNA and RNAs for HCV, MoMuLV, EMCV, FMDV and poliovirus (17–22).

ACKNOWLEDGEMENT

This work was supported in part by NIH Research Grant CA77359 from the National Cancer Institute.

REFERENCES

1. Bullock,T.N., Patterson,A.E., Franlin,L.L, Noditis,E. and Eisenlohr,L.C. (1997) *J. Exp. Med.*, **186**, 1051–1058.
2. Prats,A.C., Vagner,S., Prats,H. and Amalric,F. (1992) *Mol. Cell. Biol.*, **12**, 4796–4805.
3. Delmas,V., Laoide,B.M., Masquilier,D., de Groot,R.P., Foulkes,N.S. and Sassone-Corsi,P. (1992) *Proc. Natl Acad. Sci. USA*, **89**, 4226–4230.
4. Packham,G., Brimmell,M. and Cleveland,J.L. (1997) *Biochem. J.*, **328**, 807–813.
5. Schwartz,S., Felber,B.K., Fenyo,E.M. and Pavlakis,G.N. (1990) *J. Virol.*, **64**, 5448–5456.
6. Schwartz,S., Felber,B.K. and Pavlakis,G.N. (1992) *Mol. Cell. Biol.*, **12**, 207–219.
7. Luukkonen,B.G., Tan,W. and Schwartz,S. (1995) *J. Virol.*, **69**, 4086–4094.
8. Kozak,M. (1987) *Nucleic Acids Res.*, **15**, 8125–8148.
9. Kozak,M. (1989) *J. Cell Biol.*, **108**, 229–241.
10. Kozak,M. (1992) *Crit. Rev. Biochem. Mol. Biol.*, **27**, 385–402.
11. Kozak,M. (1986) *Cell*, **44**, 283–292.
12. Kozak,M. (1987) *J. Mol. Biol.*, **196**, 947–950.
13. Kozak,M. (1989) *Mol. Cell. Biol.*, **9**, 5073–5080.
14. Kozak,M. (1987) *Mol. Cell. Biol.*, **7**, 3438–3445.
15. Hinnebusch,A.G. (1990) *Trends Biochem. Sci.*, **15**, 148–152.
16. Kozak,M. (1995) *Proc. Natl Acad. Sci. USA*, **92**, 2662–2666.
17. Kolupaeva,V.G., Hellen,C. and Shatsky,I.N. (1996) *RNA*, **2**, 1199–1212.
18. Jang,S.K., Krausslich,H.G., Nicklin,M.J.H., Duke,J.M., Palmenberg,A.C. and Wimmer,E. (1988) *J. Virol.*, **62**, 2636–2643.
19. Pellitier,J. and Sonenberg,N. (1988) *Nature*, **334**, 320–335.
20. Kuhn,R., Luz,N. and Beck,E. (1990) *J. Virol.*, **64**, 4625–4631.
21. Tsukiyama-Kohara,K., Iizuka,N., Kohara,M. and Nomoto,A. (1992) *J. Virol.*, **66**, 1476–1483.
22. Vagner,S., Wasbort,A., Marenda,M., Gensac,M.C., Amalric,F. and Prats,A.C. (1995) *J. Biol. Chem.*, **270**, 20376–20383.
23. Nanbru,C., Lafon,I., Audigier,S., Gensac,M.C., Vagner,S., Huez,G. and Prats,A.C. (1997) *J. Biol. Chem.*, **272**, 32061–32066.
24. Hecht,S.M., Alford,B.L., Kuroda,Y. and Kitano,S. (1978) *J. Biol. Chem.*, **253**, 4517–4520.
25. Heckler,T.G., Zama,Y., Naka,T. and Hecht,S.M. (1983) *J. Biol. Chem.*, **258**, 4492–4495.
26. Heckler,T.G., Chang,L.-H., Zama,Y., Naka,T., Chorghade,M.S. and Hecht,S.M. (1984) *Biochemistry*, **23**, 1468–1473.
27. Baldini,G., Martoglio,B., Schachenmann,A., Zugliani,C. and Brunner,J., (1988) *Biochemistry*, **27**, 7951–7959.
28. Bain,J.D., Glabe,C.G., Dix,T.A., Chamberlin,A.R. and Diala,E.S. (1989) *J. Am. Chem. Soc.*, **111**, 8013–8014.
29. Roesser,J.R., Xu,C., Payne,R.C., Surratt,C.K. and Hecht,S.M. (1989) *Biochemistry*, **28**, 5185–5195.
30. Noren,C.J., Anthony-Cahill,S.J., Suich,D.J., Noren,K.A., Griffith,M.C. and Schultz,P.G. (1989) *Nucleic Acids Res.*, **17**, 9649–9660.
31. Robertson,S.A., Ellman,J.A. and Schultz,P.G. (1991) *J. Am. Chem. Soc.*, **113**, 2722–2729.
32. Hecht,S.M. (1992) *Acc. Chem. Res.*, **25**, 545–552.
33. Lodder,M., Golovine,S. and Hecht,S.M. (1997) *J. Org. Chem.*, **62**, 778–779.
34. Noren,C.J., Anthony-Cahill,S.J., Griffith,M.C. and Schultz,P.G. (1989) *Science*, **244**, 182–188.
35. Bain,J.D., Wacker,D.A., Kuo,E.E. and Chamberlin,A.R. (1991) *Tetrahedron*, **47**, 2389–2400.

36. Mamaev,S.V., Laikhter,A.L., Arslan,T. and Hecht,S.M. (1996) *J. Am. Chem. Soc.*, **118**, 7243–7244.
37. Ellman,J.A., Mendel,D. and Schultz,P.G. (1992) *Science*, **255**, 197–200.
38. Chung,H.H., Benson,D.R. and Schultz,P.G. (1993) *Science*, **259**, 806–809.
39. Mendel,D., Ellman,J.A. and Schultz,P.G. (1993) *J. Am. Chem. Soc.*, **115**, 4359–4360.
40. Thorson,J., Chapman,E., Murphy,E.C., Schultz,P.G. and Judice,J.K. (1995) *J. Am. Chem. Soc.*, **117**, 1157–1160.
41. Karginov,V.A., Mamaev,S.V., An,H., Van Cleve,M.D., Hecht,S.M., Komatsoulis,G.A. and Abelson,J.N. (1997) *J. Am. Chem. Soc.*, **119**, 8166–8176.
42. Karginov,V.A., Mamaev,S.V. and Hecht,S.M. (1997) *Nucleic Acids Res.*, **25**, 3912–3916.
43. Sanger,F., Niklen,S. and Coulson,A.R. (1977) *Proc. Natl Acad. Sci. USA*, **74**, 5463–5467.
44. Laemmli,U.K. (1970) *Nature*, **227**, 680–685.
45. Lodder,M., Golovine,S., Laikhter,A.L., Karginov,V.A. and Hecht,S.M. (1998) *J. Org. Chem.*, **63**, 794–803.
46. Varshney,U., Lee,C.-P. and RajBhandary,U.L. (1991) *J. Biol. Chem.*, **266**, 24712.
47. Sampson,J.R. and Uhlenbeck,O.C. (1988) *Proc. Natl Acad. Sci. USA*, **85**, 1033–1037.
48. Turcatti,G., Nemeth,K., Edgerton,M.D., Meseth,U., Talabot,F., Peitsch,M., Knowles,J., Vogel,H. and Chollet,A. (1996) *J. Biol. Chem.*, **271**, 19991–19998.
49. Cornish,V.W., Benson,D.R., Altenbach,C.A., Hideg,K., Hubbell,W.L. and Schultz,P.G. (1994) *Proc. Natl Acad. Sci. USA*, **91**, 2910–2914.
50. Steward,L.E., Collins,C.S., Gilmore,M.A., Carlson,J.E., Ross,J.B.A. and Chamberlin,A.R. (1997) *J. Am. Chem. Soc.*, **119**, 6–11.